

Chapter 2

Background and Preliminaries

2.1 Preliminaries

2.1.1 Notation and Definitions

In this book, \mathbb{R} denotes the set of all real numbers, the Euclidean n -dimensional space is denoted by \mathbb{R}^n , $\text{SO}(3)$ denotes the Special Orthogonal group of order three, and $\text{SE}(3)$ denotes the Special Euclidean group. A vector in \mathbb{R}^p is a column vector of dimension p , and a matrix in $\mathbb{R}^{p \times q}$ is a p -by- q matrix. The identity matrix of dimension n is denoted by \mathbf{I}_n . The vector $\mathbf{1}_n \in \mathbb{R}^n$ denotes the vector with all elements equal to one, and $\mathbf{0}_n \in \mathbb{R}^n$ denotes the vector of zero elements. The time derivative of a vector \mathbf{x} is denoted by $\dot{\mathbf{x}}$, i.e., $\dot{\mathbf{x}} = d\mathbf{x}/dt$, and moreover, $\ddot{\mathbf{x}} = d^2\mathbf{x}/dt^2, \dots$

For a vector $\mathbf{x} = (x_1, \dots, x_p)^\top \in \mathbb{R}^p$, $|\mathbf{x}| := \sqrt{\mathbf{x}^\top \mathbf{x}}$ denotes the Euclidean norm of \mathbf{x} , and $|\mathbf{x}|_\infty := \max_i |x_i|$ denotes its infinity norm, where $|x|$ is the absolute value of a scalar x . For a matrix \mathbf{A} , $\|\mathbf{A}\| := \sqrt{\lambda_m(\mathbf{A}^\top \mathbf{A})}$ denotes the induced norm of \mathbf{A} , where $\lambda_m(\mathbf{A})$ is the maximum eigenvalue of \mathbf{A} .

For time-varying functions (vectors), the \mathcal{L}_p norm is defined as

$$\|\mathbf{x}\|_p := \left(\int_0^\infty |\mathbf{x}(s)|^p ds \right)^{1/p}$$

for $p \in [1, \infty)$. The vector \mathbf{x} is said to be in \mathcal{L}_p , i.e., $\mathbf{x} \in \mathcal{L}_p$, if $\|\mathbf{x}\|_p$ is finite. Also, the notation $\mathbf{x} \in \mathcal{L}_\infty$ indicates that the \mathcal{L}_∞ norm

$$\|\mathbf{x}\|_\infty := \sup_{s \geq 0} |\mathbf{x}(s)|$$

is finite. Note that in the above definition of \mathcal{L}_2 and \mathcal{L}_∞ , $|\cdot|$ can be any norm in \mathbb{R}^n .

In addition, for clarity of presentation, the argument of all time-dependent signals (vectors) will be omitted (e.g., $\mathbf{x} \leftrightarrow \mathbf{x}(t)$), except for those that are time delayed (e.g., $\mathbf{x}(t - \tau)$), where τ denotes the time delay, which can be time-varying). Accordingly, the argument of the signals inside an integral is omitted, which is assumed to be

equal to the variable on the differential, unless otherwise stated (e.g., $\int_0^t \mathbf{x} ds \leftrightarrow \int_0^t \mathbf{x}(s) ds$). Also, the limit of a signal at infinity is replaced by an arrow (e.g., $\mathbf{x} \rightarrow 0 \leftrightarrow \lim_{t \rightarrow \infty} \mathbf{x}(t) = 0$, and $\mathbf{x} \rightarrow \mathbf{y} \leftrightarrow \lim_{t \rightarrow \infty} \mathbf{x}(t) = \lim_{t \rightarrow \infty} \mathbf{y}(t)$).

2.1.2 Useful Lemmas

Definition 2.1 [63] A function $y : [0, \infty) \rightarrow \mathbb{R}$ is said to be uniformly continuous on $[0, \infty)$ if, for any given $\varepsilon > 0$, there exists $\delta(\varepsilon) > 0$ such that $|t - t_0| < \delta(\varepsilon)$ implies $|y(t) - y(t_0)| < \varepsilon$ for all $t_0, t \in [0, \infty)$.

We give the following important lemma, which is frequently used in the analysis of control systems.

Lemma 2.1 (Barbălat Lemma [69]) *Let $y : \mathbb{R} \rightarrow \mathbb{R}$ be a uniformly continuous function on $[0, \infty)$. Suppose that $\lim_{t \rightarrow \infty} \int_0^t y(s) ds$ exists and is finite. Then,*

$$y(t) \rightarrow 0 \quad \text{as } t \rightarrow \infty. \quad (2.1)$$

An easy way of checking the uniform continuity of a function is to check the boundedness of its time derivative. In fact, a function y with bounded \dot{y} , i.e., $\dot{y} \in \mathcal{L}_\infty$, is uniformly continuous.

Lemma 2.2 *Let $y : \mathbb{R} \rightarrow \mathbb{R}$ be a continuous function defined on $[0, \infty)$. If $y(t) \rightarrow 0$ as $t \rightarrow \infty$ and $\ddot{y}(t)$ is bounded, then $\dot{y}(t) \rightarrow 0$ as $t \rightarrow \infty$.*

A special case of Barbălat lemma can be expressed as follows:

Lemma 2.3 [63] *If $y, \dot{y} \in \mathcal{L}_\infty$ and $y \in \mathcal{L}_p$ for some $p \in [0, \infty)$, then $y(t) \rightarrow 0$ as $t \rightarrow \infty$.*

An extended version of Barbălat lemma that provides less restrictive conditions is formulated in the following lemma, which can be proved, for example, following similar arguments as in the proof of Barbălat lemma in [69].

Lemma 2.4 (Extended Barbălat Lemma) *Let $x(t)$ denote a solution to the differential equation $\dot{x} = a(t) + b(t)$, with $a(t)$ a uniformly continuous function. Suppose that $x(t) \rightarrow c$ and $b(t) \rightarrow 0$ as $t \rightarrow \infty$, with c a constant value. Then,*

$$\dot{x}(t) \rightarrow 0 \quad \text{as } t \rightarrow \infty. \quad (2.2)$$

Some properties relating functions in \mathcal{L}_p are given next.

Lemma 2.5 [63] *The following is true for scalar-valued functions:*

- (i) A function $f(t)$ that is bounded from below and is nonincreasing has a limit as $t \rightarrow \infty$.
- (ii) Consider the nonnegative scalar functions $f(t)$, $g(t)$ defined for all $t \geq 0$. If $f(t) \leq g(t)$ for all $t \geq 0$ and $g \in \mathcal{L}_p$, then $f \in \mathcal{L}_p$ for all $p \in [0, \infty]$.

One of the applications of Barbălat lemma is described in the following result [132].

Lemma 2.6 *Let a scalar function $V(x, t)$ satisfy the following conditions:*

- $V(x, t)$ is lower bounded;
- $\dot{V}(x, t)$ is negative semi-definite;
- $\dot{V}(x, t)$ is uniformly continuous in time.

Then, $\dot{V}(x, t) \rightarrow 0$ as $t \rightarrow \infty$.

The following inequalities are also useful.

Lemma 2.7 (Young's inequality, [76]) *If constants $p > 1$ and $q > 1$ are such that $(p - 1)(q - 1) = 1$, then for all $\varepsilon > 0$ and for any two vectors \mathbf{x} and \mathbf{y} of the same dimension, the following inequality is satisfied:*

$$\mathbf{x}^\top \mathbf{y} \leq \frac{\varepsilon^p}{p} |\mathbf{x}|^p + \frac{1}{q \varepsilon^q} |\mathbf{y}|^q. \quad (2.3)$$

Note that the inequality in Lemma 2.7, in the case where $p = q = 2$ and $\varepsilon^2 = \kappa$, becomes

$$\mathbf{x}^\top \mathbf{y} \leq \frac{\kappa}{2} |\mathbf{x}|^2 + \frac{1}{2\kappa} |\mathbf{y}|^2. \quad (2.4)$$

Lemma 2.8 (Jensen's integral inequality, [53]) *For any positive symmetric constant matrix $\mathbf{M} \in \mathbb{R}^{n \times n}$, scalars a and b satisfying $a < b$, and a vector function $f : [a, b] \rightarrow \mathbb{R}^n$ such that the integrations concerned are well defined, we have*

$$\left(\int_a^b f \, ds \right)^\top \mathbf{M} \left(\int_a^b f \, ds \right) \leq (b - a) \int_a^b f^\top \mathbf{M} f \, ds. \quad (2.5)$$

2.1.3 Bounded Functions

In this book, we often make use of saturation functions of the elements of vectors in \mathbb{R}^3 of the form

$$\chi(\mathbf{x}) = (\sigma(x_1), \sigma(x_2), \sigma(x_3))^\top \in \mathbb{R}^3, \quad (2.6)$$

where $\mathbf{x} = (x_1, x_2, x_3)^\top \in \mathbb{R}^3$, and $\sigma : \mathbb{R} \rightarrow \mathbb{R}$ is a strictly increasing continuously differentiable function satisfying the following properties:

- P1. $\sigma(0) = 0$ and $x\sigma(x) > 0$ for $x \neq 0$,
 P2. $|\sigma(x)| \leq \sigma_b$ for $x \in \mathbb{R}$, with $\sigma_b > 0$,
 P3. The function $\frac{d\sigma(x)}{dx}$ is bounded for $x \in \mathbb{R}$.

It is worth mentioning that property P3 can be verified from P1 and P2. One example of the function σ is \tanh with $\frac{d\sigma(x)}{dx} = 1 - \tanh^2(x)$ and $\sigma_b = 1$. Other examples of scalar-valued saturation functions σ include $\arctan(x)$ and $(x/\sqrt{1+x^2})$.

The following result will be often used in the subsequent chapters and is proved in Sect. A.1.

Lemma 2.9 *Consider the second-order system*

$$\ddot{\theta} = -k_p \chi(\theta) - k_d \dot{\chi}(\theta) + \varepsilon, \quad (2.7)$$

where $\theta \in \mathbb{R}^3$, $\chi(\theta)$ is defined in (2.6), and k_p and k_d are strictly positive scalars. If ε is globally bounded and $\varepsilon \rightarrow 0$, then θ , $\dot{\theta}$ are globally bounded, and $\theta \rightarrow 0$, $\dot{\theta} \rightarrow 0$.

2.1.4 Information Flow Modeling

To achieve formation among a group of VTOL aircraft or guarantee rigid body attitude synchronization, it is necessary to design control schemes using local information exchange. Therefore, aerial vehicles need to transmit some of their states between each other. In this book, the information exchange between members of the team is described by weighted graphs. Some standard definitions and properties of graphs are given in this section, and the reader is referred, for instance, to [65] for more details.

A weighted graph \mathcal{G} consists of the triplet $(\mathcal{N}, \mathcal{E}, \mathcal{K})$ with $\mathcal{N} := \{1, \dots, n\}$ being the set of nodes or vertices, describing the set of vehicles in the group, \mathcal{E} the set of pairs of nodes, called edges, and $\mathcal{K} = [k_{ij}] \in \mathbb{R}^{n \times n}$ is a weighted adjacency matrix. An edge $(i, j) \in \mathcal{E}$ indicates that the i th system receives information from the j th system, which is designated as its neighbor. The weighted adjacency matrix of a weighted graph is defined such that $k_{ii} := 0$, $k_{ij} > 0$ if and only if $(i, j) \in \mathcal{E}$, and $k_{ij} = 0$ if and only if $(i, j) \notin \mathcal{E}$.

If the interconnection between the systems is bidirectional, then \mathcal{G} is undirected, the pairs of nodes in \mathcal{E} are unordered, i.e., $(i, j) \in \mathcal{E} \Leftrightarrow (j, i) \in \mathcal{E}$, and \mathcal{K} is symmetric, i.e., $k_{ij} = k_{ji}$. In the case of unidirectional interconnection, \mathcal{G} is a directed graph, \mathcal{E} contains ordered pairs, and \mathcal{K} is not necessarily symmetric. In graph representation, a directed edge (i, j) is represented by a directed link (arrow) leaving node j and directed toward node i . In the case of undirected graphs, links with no arrows are used.

If there is a path between any two distinct nodes of a weighted undirected graph \mathcal{G} , then \mathcal{G} is said to be *connected*. A cycle is a connected graph with each node having exactly two neighbors. “ \mathcal{G} contains a cycle” refers to a subgraph in \mathcal{G}

Fig. 2.1 Examples of undirected graphs with four nodes: (a) a connected graph, (b) a connected graph with no cycles, i.e., an undirected tree

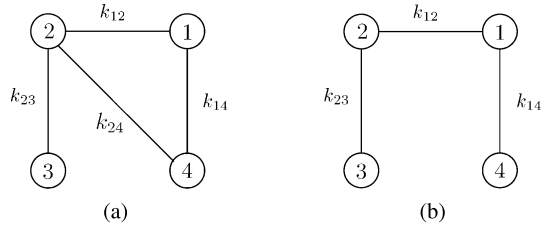
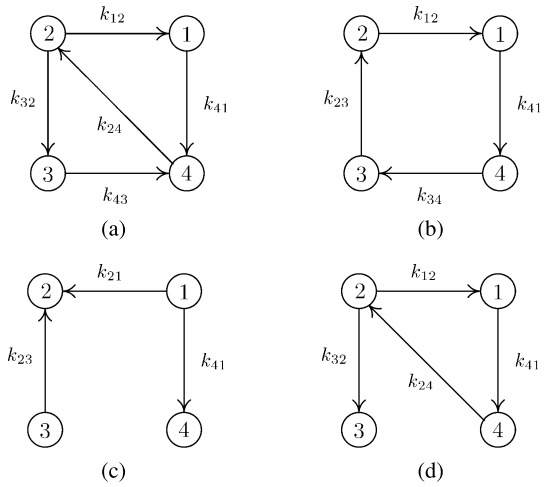


Fig. 2.2 Examples of directed graphs: (a) a strongly connected graph, (b) a strongly connected and balanced graph, (c) a weakly connected and acyclic graph, (d) a directed graph with a spanning tree



that is a cycle. An acyclic graph is a graph with no cycles. A weighted undirected graph that is connected and acyclic is called a *tree*. Figure 2.1 shows examples of undirected graphs.

A directed graph is said to be *strongly connected* if there exists a directed path between any two distinct nodes. Here, a directed path is a sequence of directed edges in a directed graph of the form $(i_1, i_2), (i_2, i_3), \dots$, where $i_l \in \mathcal{N}$. Also, for $i \in \mathcal{N}$, if the number of incoming links of node i , referred to as the in-degree of i , is equal to the number of outgoing links of node i , out-degree of i , then the graph is *balanced*. Clearly, every undirected graph is balanced. A directed graph is said to contain a directed spanning tree if there exists at least one node having a directed path to all of the other nodes. Also, a directed graph \mathcal{G} is *weakly connected* if the undirected graph \mathcal{G}' that is obtained by replacing all directed edges by undirected ones is connected. Figure 2.2 illustrates the above definitions.

The weighted incidence matrix of a directed graph $\mathcal{G} = (\mathcal{N}, \mathcal{E}, \mathcal{K})$ is denoted by $\mathbf{D} = [d_{ij}] \in \mathbb{R}^{n \times m}$, where n is the number of nodes, and m is the total number of directed edges in the graph, and is given by

$$d_{i\gamma_{\mathcal{H}}(u,v)} = \begin{cases} +k_{uv} & \text{if } i = u, \\ -k_{uv} & \text{if } i = v, \\ 0 & \text{otherwise,} \end{cases} \quad (2.8)$$

where $\mathcal{H}^{(u,v)} : \mathcal{E} \rightarrow \{1, \dots, m\}$ is a function that associates a unique number from the set $\{1, \dots, m\}$ to each directed edge $(u, v) \in \mathcal{E}$. For example, the incidence matrix of the weakly connected and acyclic directed graph in Fig. 2.2c, having the set of edges $\mathcal{E} = \{(2, 1), (2, 3), (4, 1)\}$, is given as

$$\mathbf{D} = \begin{pmatrix} -k_{21} & 0 & -k_{41} \\ k_{21} & k_{23} & 0 \\ 0 & -k_{23} & 0 \\ 0 & 0 & k_{41} \end{pmatrix}.$$

The incidence matrix \mathbf{D} satisfies the following property [65].

Property 2.1 The rank of the incidence matrix \mathbf{D} of the directed graph \mathcal{G} is $(n - 1)$ if \mathcal{G} is weakly connected, and it is full column rank if this graph is weakly connected and acyclic.

The Laplacian matrix associated to the graph $\mathcal{G} := (\mathcal{N}, \mathcal{E}, \mathcal{K})$ is denoted by $\mathbf{L} := [l_{ij}] \in \mathbb{R}^{n \times n}$ and defined as

$$l_{ii} = \sum_{j=1}^n k_{ij}, \quad l_{ij} = -k_{ij}, \quad i \neq j. \quad (2.9)$$

The Laplacian matrix of a given graph enjoys several properties that can be found in the literature of graph theory and linear multi-agent systems. Some important results used in this book are given in the following lemmas.

Lemma 2.10 (See, for instance, [61]) *Let \mathbf{L} be the Laplacian matrix associated to a directed and strongly connected graph \mathcal{G} . Then, there exists a vector $\boldsymbol{\gamma} := (\gamma_1, \gamma_2, \dots, \gamma_n)^\top \in \mathbb{R}^n$ with $\gamma_i > 0, i \in \mathcal{N}$, such that $\boldsymbol{\gamma}^\top \mathbf{L} = 0$.*

Lemma 2.11 [117] *The Laplacian matrix \mathbf{L} of a directed graph has a simple zero eigenvalue with an associated eigenvector $\mathbf{1}_n$, and all of the other eigenvalues have positive real parts if and only if the directed graph has a directed spanning tree.*

2.2 Attitude Representation and Kinematics

To represent the position and orientation of rigid-body systems, several coordinate frames are introduced. The inertial frame, denoted by \mathcal{F}_o , is rigidly attached to a point on the surface of the Earth assumed flat. The orthonormal basis associated to \mathcal{F}_o is given by the set of axes $\{\hat{e}_1, \hat{e}_2, \hat{e}_3\}$, where \hat{e}_1 points North, \hat{e}_2 points East, and \hat{e}_3 points toward the center of the Earth. The frame attached to the center of gravity (COG) of a rigid body is referred to as the body frame and is denoted by \mathcal{F}_i , where $i = b$ in the case of a single vehicle, and $i \in \mathcal{N} := \{1, \dots, n\}$ in the case of n vehicles. The basis associated to \mathcal{F}_i is given by $\{\hat{e}_{1i}, \hat{e}_{2i}, \hat{e}_{3i}\}$, where \hat{e}_{1i} is directed toward the front of the vehicle, \hat{e}_{2i} points to the right, and \hat{e}_{3i} is directed downwards.

2.2.1 Attitude Representation

The attitude of a rigid body can be described by different representations, some of which are given in this section.

2.2.1.1 Rotation Matrix

A rotation matrix \mathbf{R} describing the orientation of frame \mathcal{F}_1 with respect to frame \mathcal{F}_2 consists of the projection of the axes of \mathcal{F}_1 onto \mathcal{F}_2 . The column vectors of \mathbf{R} represent the coordinates of the axes of \mathcal{F}_1 described in \mathcal{F}_2 . Since the axes of \mathcal{F}_1 and \mathcal{F}_2 are usually unit vectors, the rotation matrix contains only cosine terms and is called the direction cosine matrix. Also, since the axes of reference frames are orthonormal, the rotation matrix is orthogonal and belongs to the set

$$\text{SO}(3) := \{\mathbf{R} \in \mathbb{R}^{3 \times 3} \mid \det(\mathbf{R}) = 1, \mathbf{R}\mathbf{R}^\top = \mathbf{R}^\top\mathbf{R} = \mathbf{I}_3\}. \quad (2.10)$$

The set $\text{SO}(3)$ forms a group with the linear matrix multiplication with identity element \mathbf{I}_3 and inverse $\mathbf{R}^{-1} = \mathbf{R}^\top$. In addition, the set $\text{SO}(3)$ offers a unique and nonsingular representation of the attitude and is generally referred to as the rotation space.

A rotation matrix can be used to map vector coordinates from one frame to another. Let $\mathbf{R} \in \text{SO}(3)$ describe the rotation from frame \mathcal{F}_1 to frame \mathcal{F}_2 . If the coordinates of a vector in \mathcal{F}_1 is denoted by \mathbf{x}_1 , then the coordinates of this vector in frame \mathcal{F}_2 is denoted by \mathbf{x}_2 , given by

$$\mathbf{x}_2 = \mathbf{R}\mathbf{x}_1. \quad (2.11)$$

The above property can be applied to the case of several frames, leading to the composition of rotations, which is obtained by the noncommutative multiplication of appropriate rotation matrices.

2.2.1.2 Euler Angles

Note that the nine elements of any rotation matrix are not independent. Therefore, it is possible to parameterize a rotation matrix $\mathbf{R} \in \text{SO}(3)$ using a smaller set of parameters. In fact, a representation of orientation can be obtained using a set of three angles, called Euler angles. The Euler angles use a combination of three subsequent rotations about some defined axes. The orientation of the body-fixed frame can then be obtained by the composition of these three rotations, provided that adjacent rotations are not made about parallel axes. As a result, 12 distinct sets of Euler angles are possible. One set of Euler angles considered in this section is (φ, θ, ψ) known as roll, pitch, and yaw angles.

The transformation that maps the vector (φ, θ, ψ) into its corresponding rotation matrix can be obtained by the successive multiplication of rotation matrices

describing the following sequence of rotations: a rotation about \hat{e}_{3b} by ψ (yaw), then a rotation about \hat{e}_{2b} by θ (pitch), followed by a rotation about \hat{e}_{1b} by φ (roll). The resulting rotation matrix describing the rotation from the inertial frame to the body-fixed frame is obtained as

$$\mathbf{R} = \begin{pmatrix} c_\theta c_\psi & c_\theta s_\psi & -s_\theta \\ s_\varphi s_\theta c_\psi - c_\varphi s_\psi & s_\varphi s_\theta s_\psi + c_\varphi c_\psi & s_\varphi c_\theta \\ c_\varphi s_\theta c_\psi + s_\varphi s_\psi & c_\varphi s_\theta s_\psi - s_\varphi c_\psi & c_\varphi c_\theta \end{pmatrix}, \quad (2.12)$$

where $c_\vartheta \equiv \cos(\vartheta)$ and $s_\vartheta \equiv \sin(\vartheta)$. The rotation matrix that describes the rotation from the body-fixed frame to the inertial frame can be obtained by taking the transpose of the above rotation matrix.

It should be noted that the roll–pitch–yaw parameterization is a minimal representation of $\text{SO}(3)$, however, it has a singularity at pitch values of $\theta = \pi/2 + k\pi$, $k \in \mathbb{Z}$. In fact, all twelve possible sets of Euler angles exhibit singularities [41, 136].

2.2.1.3 Axis–Angle Parameterization

The relative orientation of two reference frames can always be expressed by a single rotation about a given normalized vector by a given rotation angle. Let $\hat{\mathbf{k}} \in \mathbb{R}^3$ denote a unit vector, and ϑ denote the angle of rotation about $\hat{\mathbf{k}}$. Then the corresponding rotation matrix $\mathbf{R}(\vartheta, \hat{\mathbf{k}}) \in \text{SO}(3)$ is given by the following formula:

$$\mathbf{R}(\vartheta, \hat{\mathbf{k}}) = \mathbf{I}_3 - \sin(\vartheta)\mathbf{S}(\hat{\mathbf{k}}) + (1 - \cos(\vartheta))\mathbf{S}(\hat{\mathbf{k}})^2, \quad (2.13)$$

where $\mathbf{S}(\mathbf{x})$ is the skew symmetric matrix associated to $\mathbf{x} = (x_1, x_2, x_3)^\top \in \mathbb{R}^3$ given by

$$\mathbf{S}(\mathbf{x}) = \begin{pmatrix} 0 & -x_3 & x_2 \\ x_3 & 0 & -x_1 \\ -x_2 & x_1 & 0 \end{pmatrix} \quad (2.14)$$

and satisfying $\mathbf{S}(\mathbf{x})\mathbf{y} := \mathbf{x} \times \mathbf{y}$, where $\mathbf{x}, \mathbf{y} \in \mathbb{R}^3$, and “ \times ” denotes the vector cross product.

It can be seen that a rotation matrix is always defined for a given set of parameters $\{\vartheta, \hat{\mathbf{k}}\}$. However, the solution to the inverse problem, i.e., finding the set of parameters for a given rotation matrix, is not unique. This can be seen from (2.13), where $\mathbf{R}(\vartheta, \hat{\mathbf{k}}) = \mathbf{R}(-\vartheta, -\hat{\mathbf{k}})$. In addition, the case where $\mathbf{R} = \mathbf{I}_3$ leads to the solution $\{2k\pi, \hat{\mathbf{k}}\}$ for $k \in \mathbb{Z}$, for any unit-length vector $\hat{\mathbf{k}}$.

2.2.1.4 Unit Quaternion

The unit quaternion is a four-element representation of the attitude, denoted by

$$\mathbf{Q} = \begin{pmatrix} \mathbf{q} \\ \eta \end{pmatrix} \in \mathbb{Q}, \quad (2.15)$$

where $\mathbf{q} \in \mathbb{R}^3$ and $\eta \in \mathbb{R}$, and \mathbb{Q} is the set of unit quaternion defined by

$$\mathbb{Q} = \{\mathbf{Q} \in \mathbb{R}^4 \mid |\mathbf{Q}| = 1\}. \quad (2.16)$$

The unit quaternion is often considered as an axis–angle representation. Indeed, the rotation by an angle ϑ about an arbitrary unit-length vector $\hat{\mathbf{k}} \in \mathbb{R}^3$ can be described by the unit quaternion

$$\mathbf{Q} = \begin{pmatrix} \hat{\mathbf{k}} \sin(\vartheta/2) \\ \cos(\vartheta/2) \end{pmatrix}. \quad (2.17)$$

A transformation that provides a rotation matrix associated to the unit quaternion \mathbf{Q} can be obtained by the Rodrigues formula and is given by

$$\mathbf{R}(\mathbf{Q}) = (\eta^2 - \mathbf{q}^\top \mathbf{q}) \mathbf{I}_3 + 2\mathbf{q}\mathbf{q}^\top - 2\eta \mathbf{S}(\mathbf{q}), \quad (2.18)$$

where the skew symmetric matrix $\mathbf{S}(\cdot)$ is given in (2.14). It can be verified that a coordinate frame whose orientation is described by the unit quaternion \mathbf{Q} is physically equivalent to the coordinate frame whose orientation is defined by the unit quaternion $-\mathbf{Q}$. This can be easily verified from (2.18) where $\mathbf{R}(\mathbf{Q}) = \mathbf{R}(-\mathbf{Q})$. Also, it can be seen from (2.17) that

$$-\mathbf{Q} = \begin{pmatrix} -\hat{\mathbf{k}} \sin(\vartheta/2) \\ -\cos(\vartheta/2) \end{pmatrix} = \begin{pmatrix} \hat{\mathbf{k}} \sin((\vartheta + 2k\pi)/2) \\ \cos((\vartheta + 2k\pi)/2) \end{pmatrix} \quad (2.19)$$

for $k \in \mathbb{Z}$, which indicates that the difference between \mathbf{Q} and $-\mathbf{Q}$ resides in the angle ϑ , which is increased by a value of $2k\pi$. Therefore, if the orientation of two different frames of interest are described by the unit quaternions \mathbf{Q} and $-\mathbf{Q}$, respectively, the orientation of the two coordinate frames are physically equivalent and have the same value for the rotation matrix using the $\text{SO}(3)$ parameterization.

Analogous to linear matrix multiplication of rotation matrices, the composition of successive rotations represented by a unit quaternion is obtained by the distributive and associative, but not commutative, quaternion multiplication. To define this operation, consider two unit quaternion

$$\mathbf{Q}_1 = \begin{pmatrix} \mathbf{q}_1 \\ \eta_1 \end{pmatrix}, \quad \mathbf{Q}_2 = \begin{pmatrix} \mathbf{q}_2 \\ \eta_2 \end{pmatrix}.$$

The quaternion product between \mathbf{Q}_1 and \mathbf{Q}_2 , denoted by $\mathbf{Q}_3 \in \mathbb{Q}$, is given by

$$\mathbf{Q}_3 = \mathbf{Q}_1 \odot \mathbf{Q}_2 = \begin{pmatrix} \eta_1 \mathbf{q}_2 + \eta_2 \mathbf{q}_1 + \mathbf{S}(\mathbf{q}_1) \mathbf{q}_2 \\ \eta_1 \eta_2 - \mathbf{q}_1^\top \mathbf{q}_2 \end{pmatrix}, \quad (2.20)$$

and the rotation matrix associated to \mathbf{Q}_3 is obtained as $\mathbf{R}(\mathbf{Q}_3) = \mathbf{R}(\mathbf{Q}_2) \mathbf{R}(\mathbf{Q}_1)$. The set of unit quaternion \mathbb{Q} forms a group with the quaternion multiplication \odot and with the quaternion inverse

$$\mathbf{Q}^{-1} := \begin{pmatrix} -\mathbf{q} \\ \eta \end{pmatrix} \in \mathbb{Q} \quad (2.21)$$

such that

$$\mathbf{Q} \odot \mathbf{Q}^{-1} = \mathbf{Q}^{-1} \odot \mathbf{Q} = \mathbf{Q}_I, \quad (2.22)$$

where \mathbf{Q}_I is the identity quaternion, which can be viewed as a rotation by a zero angle about an arbitrary vector of rotation and is given by

$$\mathbf{Q}_I := \begin{pmatrix} \mathbf{0}_3 \\ 1 \end{pmatrix}. \quad (2.23)$$

Using (2.18) and (2.21), it is clear that $\mathbf{R}(\mathbf{Q}^{-1}) = \mathbf{R}(\mathbf{Q})^\top$.

Using the quaternion product, the unit quaternion can also be used to give the coordinates of a vector in multiple frames of reference similar to (2.11). In fact, having the property $\mathbf{x}_2 = \mathbf{R}(\mathbf{Q})\mathbf{x}_1$, the vector \mathbf{x}_2 can also be obtained using the quaternion product by the following operation:

$$\begin{pmatrix} \mathbf{x}_2 \\ 0 \end{pmatrix} = \mathbf{Q}^{-1} \odot \begin{pmatrix} \mathbf{x}_1 \\ 0 \end{pmatrix} \odot \mathbf{Q}. \quad (2.24)$$

2.2.1.5 Rodrigues Parameters

The Rodrigues vector is another representation of the attitude and is derived from the definition of the unit quaternion \mathbf{Q} in (2.17) as [130]

$$\boldsymbol{\rho} := \frac{1}{\eta} \mathbf{q} = \hat{k} \tan(\vartheta/2), \quad (2.25)$$

where the three elements of $\boldsymbol{\rho}$ are known as the Rodrigues parameters. The rotation matrix associated to $\boldsymbol{\rho}$ can be obtained from (2.18) by noting that [130]

$$\mathbf{Q} = \frac{1}{\sqrt{1 + |\boldsymbol{\rho}|^2}} \begin{pmatrix} \boldsymbol{\rho} \\ 1 \end{pmatrix}. \quad (2.26)$$

The Rodrigues parameters representation uses only three elements and hence is minimal. However, the Rodrigues vector cannot be used to represent rotations through $\pm\pi$, which correspond to $\eta = 0$. A different but related representation to the Rodrigues parameters is the modified Rodrigues parameters (MRP) representation. The MRPs are the elements of the vector $\bar{\boldsymbol{\rho}}$ defined as

$$\bar{\boldsymbol{\rho}} := \frac{1}{1 + \eta} \mathbf{q} = \hat{k} \tan(\vartheta/4). \quad (2.27)$$

It is clear that the MRP representation of the attitude is also minimal; however, the modified Rodrigues vector is not defined for $\eta = -1$. This indicates that the singularity has moved to $\pm 2\pi$ as compared to the Rodrigues vector.

2.2.1.6 Comparison of Attitude Representations

From the above subsections we can see that the three-element representation of the attitude is not global. The set of roll–pitch–yaw, for instance, is only suitable for vehicles that do not perform vertical maneuvers, such as land vehicles, ships, and transport aircraft [41]. Also, other three-elements representations derived using the unit quaternion, such as the Rodrigues parameters or the MRP are geometrically singular. If the rotation angle is restricted to be less than 2π for instance, the MRPs provide a continuous and unique representation of the orientation. However, if the rotation angle is not bounded, it is not possible to avoid the singularity using such a representation.

In contrast, all attitudes of a rigid body can be described using four-element representations, i.e., axis–angle and unit-quaternion representations, and rotation matrices; however, only rotation matrices provide a unique representation of all attitudes [33]. Despite this fact, the unit-quaternion representation is often used in practical applications to represent the attitude of a rigid body due to some significant advantages it offers over $SO(3)$ representation [149]. In fact, unit quaternions often provide simplified analysis and design of control systems as compared to methods relying on rotation matrices. In addition, the rotation matrix associated to a unit quaternion, given in (2.18), is computationally efficient. For these reasons, we consider in this book the unit quaternion to represent the attitude of a rigid body.

It is worth pointing out that the unit-quaternion representation is nonminimal and, as such, is an over-parameterization of the rotation space $SO(3)$. In fact, the transformation $\mathbb{Q} \rightarrow SO(3)$ is a two-to-one map. Therefore, when using this representation, a problem arises in the control design and analysis since for every equilibrium solution that exists in the real motion space, two equilibrium solutions exist in the quaternion space. Note that although these two equilibrium solutions correspond to the same physical configuration of the rigid body, they do not necessarily share the same mathematical properties. In fact, this pair of equilibria can have completely different characteristics, such as one being an attractor while the other being a repeller. This causes the unwinding effect, where trajectories starting near a desired equilibrium solution can diverge and travel a large distance before coming back to the same equilibrium solution. This and other cases are discussed in [29, 33], and [71].

2.2.2 Attitude Kinematics

Let $\mathbf{Q} \in \mathbb{Q}$ be the unit quaternion that describes the orientation of the body-fixed frame with respect to the inertial frame. Also, let $\boldsymbol{\omega} \in \mathbb{R}^3$ be the angular velocity of the body frame with respect to the inertial frame, expressed in the body frame (body-referenced angular velocity). The time derivative of the rotation matrix $\mathbf{R}(\mathbf{Q})$ associated to \mathbf{Q} , defined in (2.18), can be obtained as

$$\dot{\mathbf{R}}(\mathbf{Q}) = -\mathbf{S}(\boldsymbol{\omega})\mathbf{R}(\mathbf{Q}), \quad (2.28)$$

where $\mathbf{S}(\cdot)$ is the skew symmetric matrix defined in (2.14). The kinematic differential equation of the rigid body attitude can be obtained as [130]

$$\dot{\mathbf{Q}} = \frac{1}{2} \mathbf{T}(\mathbf{Q}) \boldsymbol{\omega}, \quad (2.29)$$

with $\mathbf{T}(\mathbf{Q})$ given by

$$\mathbf{T}(\mathbf{Q}) = \begin{pmatrix} \eta \mathbf{I}_3 + \mathbf{S}(\mathbf{q}) \\ -\mathbf{q}^\top \end{pmatrix}, \quad (2.30)$$

and satisfies $\mathbf{T}(\mathbf{Q})^\top \mathbf{T}(\mathbf{Q}) = \mathbf{I}_3$. Therefore, the inverse kinematic problem can be solved as

$$\boldsymbol{\omega} = 2\mathbf{T}(\mathbf{Q})^\top \dot{\mathbf{Q}}. \quad (2.31)$$

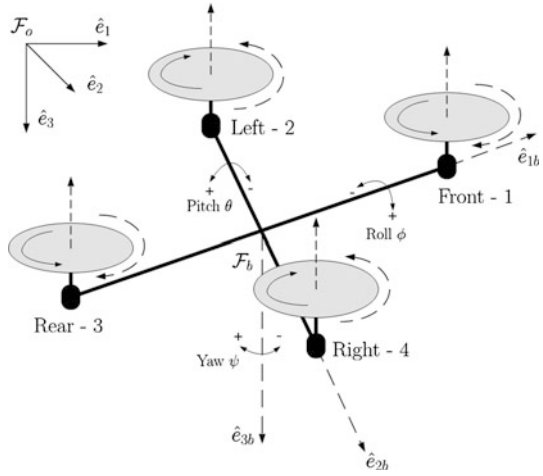
2.3 Dynamical Model of VTOL UAVs

In this section, the equations of motion for unmanned aerial vehicles capable of vertical take-off and landing are presented. Let the position and linear velocity of the COG of the aerial vehicle expressed in \mathcal{F}_o be denoted, respectively, by $\mathbf{p} \in \mathbb{R}^3$ and $\mathbf{v} \in \mathbb{R}^3$. Let the orientation of the body fixed frame be represented by the unit quaternion \mathbf{Q} , and let $\boldsymbol{\omega}$ be the body-referenced angular velocity of the aircraft. Also, let $\mathbf{R}(\mathbf{Q})$ denote the rotation matrix associated to \mathbf{Q} that brings the inertial frame into the body frame. Furthermore, let m and g denote respectively the mass of the aircraft and the acceleration due to gravity, and $\mathbf{J} \in \mathbb{R}^{3 \times 3}$ denote the symmetric positive definite constant inertia matrix of the body with respect to \mathcal{F}_b . With this notation, we consider the dynamic model of two different VTOL aircraft and then give a nominal model for this class of VTOL UAVs used in the subsequent developments.

2.3.1 Example of Quadrotor Aircraft

An example of a thrust-propelled VTOL aerial vehicle is the quadrotor aircraft, which is most common due to its simplicity. This aircraft consists of a rigid cross airframe with four individual rotors as seen in Fig. 2.3. The front and rear rotors, numbered 1 and 3, rotate counterclockwise (positive about the z -axis), while the left and right rotors, numbered 2 and 4, rotate in a clockwise direction. Vertical motion is achieved by increasing or decreasing the speed of each rotor by the same proportion. The roll motion is controlled by increasing the thrust of rotor 2 (4) and decreasing the thrust of rotor 4 (2) to obtain a positive (negative) roll to the right (left). The pitch motion is achieved similarly by differential speed between rotors 1 and 3. The yaw motion of the quadrotor is achieved by adjusting the average thrust of the clockwise and counterclockwise rotating rotors. When a yaw motion in the

Fig. 2.3 Frames and notation for the quadrotor model



positive direction is desired for example, the rotor pair 1 and 3 increase by the same proportion, while the rotor pair 2 and 4 decrease by the same proportion. This will maintain the same overall aircraft thrust without pitching or rolling the aircraft.

The equations of motion of the quadrotor aircraft can be derived as [141]

$$\begin{aligned}
 \dot{\mathbf{p}} &= \mathbf{v}, \\
 m\dot{\mathbf{v}} &= mg\hat{e}_3 - \mathcal{T}\mathbf{R}(\mathbf{Q})^\top \hat{e}_3, \\
 \dot{\mathbf{Q}} &= (1/2)\mathbf{T}(\mathbf{Q})\boldsymbol{\omega}, \\
 \mathbf{J}\dot{\boldsymbol{\omega}} &= \boldsymbol{\Gamma} - \mathbf{S}(\boldsymbol{\omega})\mathbf{J}\boldsymbol{\omega} - \mathbf{G}_a,
 \end{aligned} \tag{2.32}$$

with

$$\mathbf{J}_r \dot{\omega}_i = \mathbf{v}_i - W_i, \quad i \in \{1, 2, 3, 4\}, \tag{2.33}$$

where $\hat{e}_3 := (0, 0, 1)^\top$ denotes the unit vector in the coordinate frame \mathcal{F}_o , and the moment of inertia and speed of the rotors are denoted, respectively, by \mathbf{J}_r and ω_i , $i \in \{1, 2, 3, 4\}$. The vector \mathbf{G}_a contains the gyroscopic torques due to the combination of the rotation of the airframe and the four rotors and is given by [141]

$$\mathbf{G}_a = \sum_{i=1}^4 (-1)^{i+1} \mathbf{J}_r \mathbf{S}(\boldsymbol{\omega}) \hat{e}_3 \omega_i, \tag{2.34}$$

and the reactive torque acting on the airframe due to rotor drag generated by the i th rotor, in free air, is denoted by W_i and can be modeled as $W_i := \kappa \omega_i^2$ with $\kappa > 0$. The positive scalar \mathcal{T} denotes the total thrust applied to the airframe by the four rotors in the direction of \hat{e}_{3b} , and $\boldsymbol{\Gamma} \in \mathbb{R}^3$ is the external torque applied to the airframe by the four rotors expressed in \mathcal{F}_b . The expression relating $(\mathcal{T}, \boldsymbol{\Gamma}^\top)^\top$ and

the speed of the rotors in a quadrotor can be obtained in the following matrix form:

$$\begin{pmatrix} \mathcal{T} \\ \Gamma \end{pmatrix} = \begin{pmatrix} b & b & b & b \\ 0 & bd & 0 & -bd \\ -bd & 0 & bd & 0 \\ \kappa & -\kappa & \kappa & -\kappa \end{pmatrix} \begin{pmatrix} \varpi_1^2 \\ \varpi_2^2 \\ \varpi_3^2 \\ \varpi_4^2 \end{pmatrix} := \mathbf{M} \begin{pmatrix} \varpi_1^2 \\ \varpi_2^2 \\ \varpi_3^2 \\ \varpi_4^2 \end{pmatrix}, \quad (2.35)$$

where d represents the distance between the rotor to the COG of the aircraft, κ and $b > 0$ are parameters depending on the density of air, the size, shape, and pitch angle of the blades, as well as other factors [89, 90, 109]. Note that for $\kappa bd \neq 0$, the matrix \mathbf{M} is nonsingular. For a given desired thrust and input torque, the desired speed of each rotor can be obtained from (2.35).

To control the quadrotor aircraft, Eqs. (2.32) can be considered to design appropriate thrust and torque inputs. Then, for a given desired speed of each rotor determined from (2.35), the input voltage v_i for each motor can be designed from (2.33) to track the desired speed.

2.3.2 Example of Ducted-Fan Aircraft

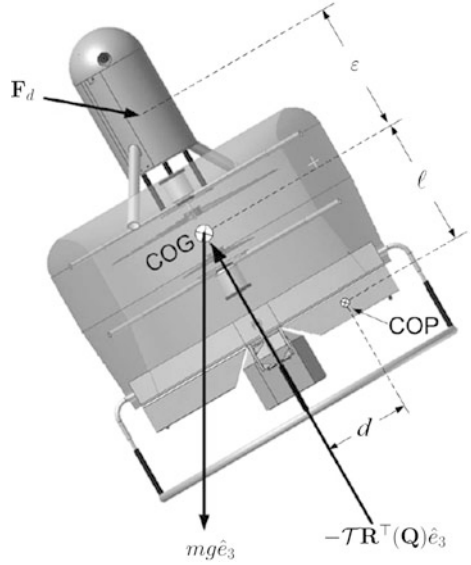
A ducted fan, in aerospace applications, is usually attributed to a special configuration where the rotor (propeller) is surrounded by a shroud (duct). This configuration which is interesting for its safety features, is also attractive for small VTOL UAVs as it provides increased thrust efficiency at low velocities [121]. The ducted fan is somewhat more popular in small-scale VTOL UAVs, and a number of research groups have used this system as an experimental platform [107, 121].

These systems are usually actuated with one or two coaxial propellers, generating the required thrust, and ailerons or control surfaces, at the exit of the duct, controlling the orientation of the UAV. A simplified dynamical model of a ducted-fan VTOL-UAV equipped with two coaxial propellers and four servo-actuated ailerons is given by [122]

$$\begin{aligned} \dot{\mathbf{p}} &= \mathbf{v}, \\ m\dot{\mathbf{v}} &= mg\hat{e}_3 - \mathcal{T}\mathbf{R}(\mathbf{Q})^\top \hat{e}_3 - \frac{1}{l}\mathbf{R}(\mathbf{Q})^\top \mathbf{S}(\hat{e}_3)\Gamma + \mathbf{R}(\mathbf{Q})^\top \mathbf{F}_d, \\ \dot{\mathbf{Q}} &= (1/2)\mathbf{T}(\mathbf{Q})\boldsymbol{\omega}, \\ \mathbf{J}\dot{\boldsymbol{\omega}} &= -\mathbf{S}(\boldsymbol{\omega})\mathbf{J}\boldsymbol{\omega} + \Gamma + \varepsilon\mathbf{S}(\hat{e}_3)\mathbf{F}_d, \end{aligned} \quad (2.36)$$

where the external disturbances due to the aerodynamic drag and wind gusts are represented by an unknown body-referenced force \mathbf{F}_d applied at an unknown distance ε from the COG of the vehicle as shown in Fig. 2.4. The distance l between the COG and the aileron center of pressure (COP), as shown in Fig. 2.4, represents the torque lever arm. A model for \mathbf{F}_d can be found in [121, 122]. Note that the above

Fig. 2.4 Model of a ducted-fan UAV



model is obtained by assuming that the two rotors rotate at the same speed and in opposite directions.

The thrust generated by the rotors is given by

$$\mathcal{T} = \kappa_{\mathcal{T}} \boldsymbol{\omega}_r^2, \quad (2.37)$$

where $\boldsymbol{\omega}_r$ is the speed of the rotors, and $\kappa_{\mathcal{T}}$ is a parameter depending on the density of air, the rotors, and other factors [121]. The airframe torque is generated through the deflection of air by the four ailerons and can be modeled as

$$\boldsymbol{\Gamma} = \kappa_L \mathcal{T} \begin{pmatrix} -l & -l & 0 & 0 \\ 0 & 0 & -l & -l \\ -d & d & -d & d \end{pmatrix} \begin{pmatrix} \alpha_1 \\ \alpha_2 \\ \alpha_3 \\ \alpha_4 \end{pmatrix}, \quad (2.38)$$

where α_i is the angle of attack of aileron i , $i \in \{1, 2, 3, 4\}$, and κ_L is a lift constant depending on the size, shape of the aileron, and other parameters [121].

Similar to the quadrotor, the control design for the ducted-fan UAV can be performed by considering (2.36) to determine appropriate thrust and torque inputs to achieve the control objectives. Then, Eqs. (2.37) and (2.38) can be used to determine the desired speed of the rotors and the angles of attack of the ailerons.

2.3.3 Nominal Model for VTOL UAVs

The nominal dynamical model of VTOL UAVs considered in this book is given as follows.

Translational Dynamics:

$$\begin{aligned}\dot{\mathbf{p}} &= \mathbf{v}, \\ \dot{\mathbf{v}} &= g\hat{e}_3 - \frac{\mathcal{T}}{m}\mathbf{R}(\mathbf{Q})^\top \hat{e}_3.\end{aligned}\tag{2.39}$$

Rotational Dynamics:

$$\begin{aligned}\dot{\mathbf{Q}} &= \frac{1}{2}\mathbf{T}(\mathbf{Q})\boldsymbol{\omega}, \\ \mathbf{J}\dot{\boldsymbol{\omega}} &= \boldsymbol{\Gamma} - \mathbf{S}(\boldsymbol{\omega})\mathbf{J}\boldsymbol{\omega},\end{aligned}\tag{2.40}$$

where $\hat{e}_3 := (0, 0, 1)^\top$, and \mathcal{T} and $\boldsymbol{\Gamma}$ are, respectively, the thrust and torque inputs applied to the aircraft.

The nominal dynamical model (2.39)–(2.40) is obtained by assuming negligible aerodynamic and external disturbances. This nominal model is obtained from the quadrotor equations of motion (2.32) assuming a negligible gyroscopic torque G_a . Note that the gyroscopic torque is a passive term in the sense that it does not contribute to the variation of the rotational kinetic energy of the UAV and can be handled quite easily in the control design. Also, in near hover-conditions (i.e., small pitch and roll), it is commonly assumed that $G_a \approx 0$. On the other hand, the nominal dynamical model is obtained from the ducted-fan model (2.36) assuming that $\varepsilon \approx 0$, $ml \gg 1$, and $\mathbf{F}_d \approx 0$, which is a common assumption when dealing with the control design for ducted-fan UAVs.

It is clear that the VTOL UAV is an under-actuated system since the force responsible for the translational motion is generated in a single direction, and the two other components of the position vector cannot be “directly” controlled. Note that Eqs. (2.40) describe the attitude dynamics of a rotating rigid body in a three-dimensional space, and $\boldsymbol{\Gamma}$ represents the torque applied around the three primary axes of rotation.

Motion Coordination for VTOL Unmanned Aerial Vehicles

Attitude Synchronisation and Formation Control

Abdessameud, A.; Tayebi, A.

2013, XV, 182 p., Hardcover

ISBN: 978-1-4471-5093-0